International Journal of Environmental Sciences
ISSN: 2229-7359
Vol. 11 No. 4, 2025
https://theaspd.com/index.php

Landslide Susceptibility Mapping Using Frequency Ratio And Dempster-Shafer Theory For Palakkad District, Kerala, India

Mohana Devi M [1], Evany Nithya S [2], Jegan J [3]
[1] P.G. Student, Department of Civil Engineering, University College of Engineering, Bit Campus, Anna University, Tiruchirappalli – 620 024, Tamilnadu, India, mmohanadevi10@gmail.com
[2] Assistant Professor, Department of Civil Engineering, University College of Engineering, Bit Campus, Anna University, Tiruchirappalli – 620 024, Tamilnadu, India, Orcid Id: 0000-0001-6196-0353, evanynithya@aubit.edu.in
[3] Professor, Department of Civil Engineering, University College of Engineering, Bit Campus, Anna University, Tiruchirappalli – 620 024, Tamilnadu, India, Orcid Id: 0000-6727-1567, jegan@aubit.edu.in

Abstract
Landslides are a significant natural hazard in the Palakkad district of Kerala, India, causing widespread damage to life and property. This study aims to develop a landslide susceptibility map (LSM) for the region using the Frequency Ratio (FR) and Dempster-Shafer Theory of Evidence (DST) models. A comprehensive landslide inventory map was prepared, consisting of 593 landslide locations, which were divided into two subsets: 70% for model training and 30% for validation. The analysis incorporated several landslide causative factors including slope, aspect, drainage density, rainfall, geology, geomorphology, soil, land use/land cover, curvature, and road network density. These factors were integrated into Geographic Information System (GIS) platforms to produce LSMs using both the FR and DST models. The model validation was conducted using receiver operating characteristic (ROC) curves. The results demonstrated that the FR model achieved an accuracy of 85%, while the DST model exhibited a higher prediction accuracy of 95%. This highlights the superior performance of the DST model in predicting landslide prone areas. The finding provides valuable insights for disaster management and planning in the Palakkad district. The DST-based LSM, with its high predictive capability, can serve as a reliable tool for mitigating landslide risks and guiding sustainable land-use planning in the region.

Keywords *- Landslide susceptibility, Frequency Ratio, Dempster-Shafer Theory of Evidence, GIS, Palakkad district*

1. INTRODUCTION

Landslides are catastrophic geohazards that occur due to the interplay of natural and anthropogenic factors, causing severe socio-economic and environmental impacts globally. Landslide causative factors include topographical parameters (slope, aspect, curvature), geological and geomorphological characteristics, hydrological factors (drainage density and rainfall intensity), soil properties and human activities (deforestation, mining, and infrastructure development) (Guzzetti et al., 2005). The intricate interaction of these factors underlies the complexity of landslide susceptibility assessments.

India is one of the most affected countries by landslides with Himalayas and the Western Ghats experiencing high frequencies due to their unique topographical and climatic conditions. In the Himalayas, active tectonics, steep slopes and high precipitation contribute to significant landslide activity (Dai et al., 2002). In Western Ghats a UNESCO World Heritage site, heavy monsoonal rainfall, fragile lateritic soils and deforestation are primary contributors (Aleotti & Chowdhury, 1999). The monsoon season (June–September) is particularly critical, with rainfall-induced landslides causing widespread disruptions annually.The Palakkad district, located within the Western Ghats, is highly susceptible to landslides due to its rugged terrain, high rainfall and unregulated anthropogenic activities (Sarkar et al., 2012). Past landslide events in the region have resulted in considerable loss of life, destruction of property and long-term impacts on local livelihoods (Chen et al., 2017). To mitigate these risks, it is essential to develop an accurate landslide susceptibility maps (LSMs).

Remote Sensing (RS) and Geographic Information Systems (GIS) have emerged as critical tools in landslide investigations. RS provides high-resolution and multi-temporal data essential for identifying

landslide-prone areas, while GIS enables the integration and spatial analysis of diverse datasets (Pradhan, 2010; Westen et al., 2008). By combining these technologies, comprehensive landslide susceptibility map can be created to support disaster risk management. This study employs two widely recognized modeling approaches for landslide susceptibility mapping: the Frequency Ratio (FR) and Dempster-Shafer Theory of Evidence (DST). The frequency ratio model evaluates the correlation between landslide occurrences and causative factors by calculating statistical likelihoods (Pourghasemi et al., 2012). Dempster-Shafer Theory of Evidence, a probabilistic framework, integrates multiple sources of evidence to estimate the likelihood of landslides, offering a more robust prediction mechanism (Chen et al., 2017).Model performance is validated using the Area Under the Curve (AUC) of Receiver Operating Characteristic (ROC) curves. The AUC-ROC method quantitatively evaluates the model accuracy in predicting landslide-prone areas, enabling a comparative assessment of FR and DST (Lee & Talib, 2005). This investigation work aims to enhance the understanding of landslide susceptibility in the Palakkad district by leveraging advanced geospatial tools and statistical models. The findings will contribute to sustainable land-use planning and disaster risk reduction strategies, addressing the challenges posed by landslides in the vulnerable region.

2. STUDY AREA

Palakkad District, located in the central part of Kerala, India, spans an area of approximately 4,480 km^2 and is home to a population exceeding 2.8 million (Fig.1) (Shibu & Nair, 2016). Geographically, the district is situated between the Western Ghats and Tamil Nadu, with topographical variations ranging from steep hills and valleys in the west to gentler plains in the east (Sreekumar et al., 2017). The region experiences a tropical monsoon climate, receiving heavy rainfall from June to September, which significantly contributes to landslide vulnerability, especially in the hilly areas (Nair & Srinivasan, 2020). Major landslide prone zones in the district include the Nelliampathy Hills, Attappady and other regions along the Western Ghats, where steep slopes and heavy monsoonal rains are common triggers (Menon et al., 2018).

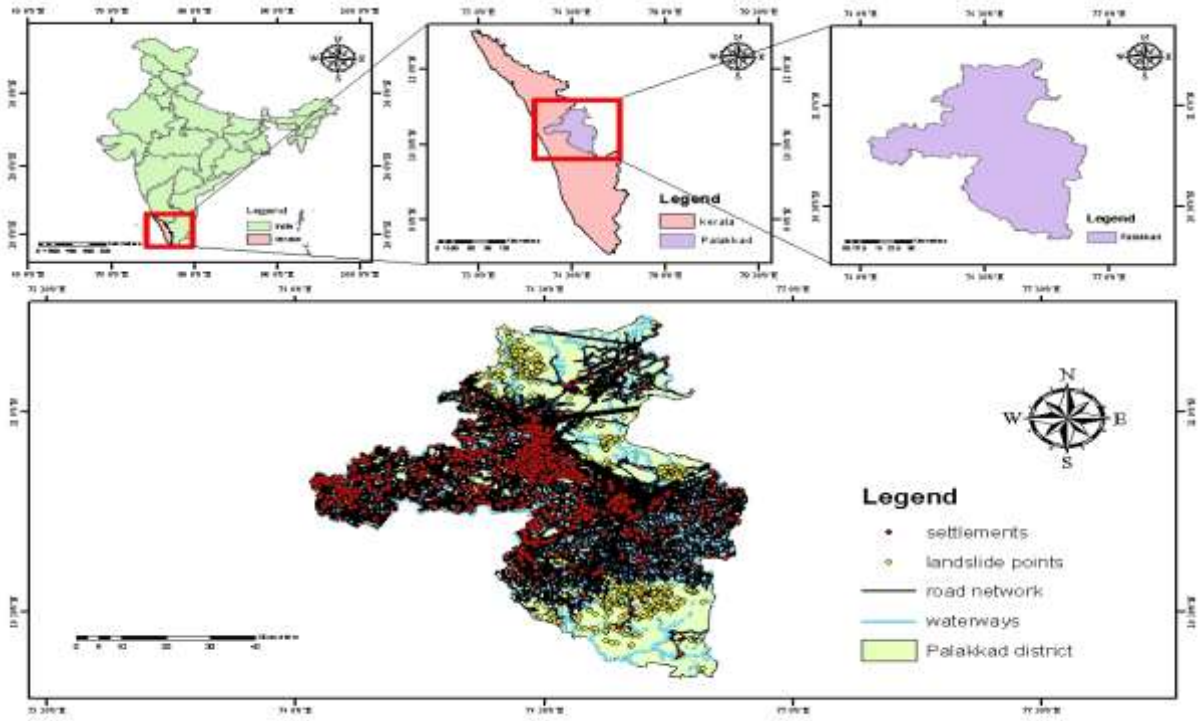

Fig.1 Study Area (Palakkad district, Kerela)

Geologically, Palakkad is underlain by precambrian rocks such as granite, gneiss, and schist, which are susceptible to weathering and erosion, thereby heightening the risk of landslides (Sreekumar et al., 2017). These geological characteristics, combined with heavy rainfall and hydrological factors, create conditions

conducive to frequent slope failures during the monsoon season (Thomas et al., 2015). The Western Ghats play a pivotal role in shaping the district's climate and hydrological dynamics, further influencing landslide occurrences (Menon et al., 2018). In particular, poorly consolidated soils and fractured bedrock in the region make slopes prone to instability under intense precipitation (Paul & Mathew, 2019).Anthropogenic activities such as urbanization, deforestation and infrastructure development have exacerbated the landslide risk in Palakkad. The construction of roads, agricultural expansion and deforestation in steep terrains has altered natural drainage patterns and destabilizes the slopes (Vinod & Shetty, 2021). These changes, coupled with increased soil erosion and surface runoff, have intensified landslide susceptibility in the district (Gupta & Rajagopal, 2019). Consequently, the preparation of a detailed landslide susceptibility map for Palakkad is critical in disaster risk reduction, informed land-use planning, and implementing effective mitigation strategies (Shibu & Nair, 2016). Figure 2 shows the schematic representation of proposed Landslide Susceptibility Mapping for Palakkad district.

3. DATA USED FOR THEMATIC MAP PREPARATION

Satellite imagery and DEM data play crucial roles in geospatial analysis for assessing slope stability and erosion potential. Landsat 8 satellite imagery, sourced from Earth Explorer, offers a 30-meter resolution, balancing spatial coverage and detail for regional studies. This imagery provides critical land-use and land-cover information, including vegetation, built-up areas and bare land. Complementing this, the SRTM DEM with a 30-meter resolution is pivotal for terrain analysis, offering detailed attributes such as slope, aspect, curvature and drainage density. These parameters are instrumental in evaluating terrain stability and the susceptibility of regions to landslides. Rainfall data from Nasa Power spans a decade (2012–2022), with temporal resolution enabling the identification of trends and anomalies linked to landslides. Soil data from the Food and Agricultural Organization (FAO) Soils Portal highlights the texture and composition, necessary for evaluating slope stability under heavy rainfall. Road data from BBBike Extract quantifies the influence of infrastructure on natural slopes, with proximity intervals of 100m, 150m, and 200m. Geological data from BhuKosh provides insights into lithology, geomorphology and structural features, enhancing understanding of terrain mechanics and rock type differentiation through RGB-coded litho units. Together, these datasets offer a comprehensive foundation for landslide risk assessment and terrain stability studies.

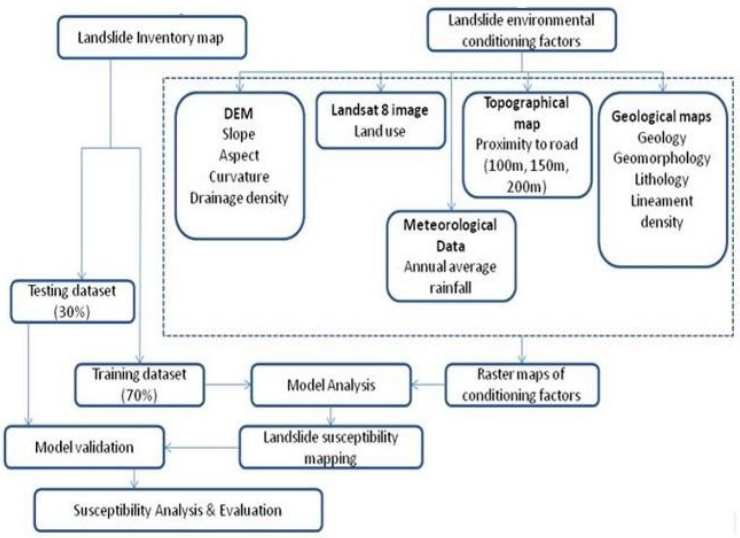

Fig.2. Schematic representation of proposed LSM

3.1. Landslide inventory map

The landslide inventory is a database of past landslide events in the study area. It includes spatial locations of historical landslides. This data is critical for training and testing the susceptibility models as it explains the relationship between environmental factors and landslide occurrences. The landslide locations were

collected from government records and satellite images. A total of 848 landslides were identified for the study area. Seventy percentage (593) of the landslides are selected for training the models and thirty percentage (255) of the landslides are used for validation.

4. Thematic map preparation

To predict the landslide susceptibility areas different causative factors were selected after carefully analyzing the study area. The factors selected for predictive analysis of landslide susceptibility for the Palakkad district are slope, aspect, drainage density, rainfall, geology, geomorphology, soil, land use/land cover, curvature and road network density. Thematic maps were prepared for the landslide causative factors. Figure 3 shows the thematic maps for the respective landslide conditioning factors.

4.1. Slope: Slope map depicts the steepness of terrain, which directly influences gravitational forces acting on slopes, making steeper areas more susceptible to landslides (Ayalew et al., 2004). The slope was mapped using DEM data using the surface tool in spatial analysis. Slope map is classified as Very gentle (0 - 3 %), Gentle (3 - 8 %), Moderate (8 - 18 %), Moderately steep (18 - 30%), Steep (30 - 50%), Very steep > (50 %) and it is vital for identifying high-risk zones.

4.2. Aspect: Aspect map shows the slope direction, sunlight exposure, vegetation growth and soil moisture, all of which affects slope stability (Regmi et al., 2014). Aspect map was prepared by setting the DEM as an input to surface tool in spatial analysis in ArcGIS. The classes present in aspect are flat, north, northeast, east, southeast, south, southwest, west, northwest. Soil moisture and sunlight exposure influences the vegetation growth which affects the slope stability by its root network. Thus aspect is critical in understanding the localized landslide susceptibility.

4.3. Drainage Density: Drainage density map measures the sum of the channel lengths per unit area, indicating water flow and erosion potential. Streams are derived by giving DEM as input to flow direction and flow accumulation tool. Then hydrology tool in spatial analysis is used to get the drainage lines. The line density tool is used to create the drainage density map. The drainage density is classified using natural break in to three classes as low, medium and high. High drainage density increases the slope saturation and soil erosion and thereby increases the landslide risk (Gokceoglu & Aksoy, 1996).

4.4. Rainfall: Rainfall map identifies regions with high precipitation, which act as a triggering factor for landslides (Crozier, 2010). The rainfall data is collected from the 10 rain gauge stations (Parambikulam, Kollengode, Alathur, Erimayur, Chittur, Palakkad, Ottapalam, Pattambi, Thrithala, Mannarkad). The rainfall data was given as input and Inverse Distance Weighted method is used to interpret the data to generate rainfall map. Rainfall map is classified into 3 classes as low (1600-2030 mm), medium (2031-2300 mm) and high (2301-2800 mm).

4.5. Geology: Geological map provides information on lithology and structural features, highlighting zones with weak or fractured rock formations prone to failure (Soeters & van Westen, 1996). Geology map was directly obtained from the BhuKosh. The geology of the area is classified as Satyamangalam gp., Peninsular gneissic complex-I, Migmatite gneissic complex (southern granulite terrain), Charnockite gneissic complex (southern granulite terrain), Khondalite gneissic complex (southern granulite terrain), Acid intrusive / granite / granodiorite, Undiff.fluvial / aeolian / coasta & glacial sediments.

4.6. Geomorphology: Geomorphology map categorizes landforms and surface processes, emphasizing zones of active erosion or deposition, which influence landslide dynamics. The map was obtained from the BhuKosh. BhuKosh is the gateway for all the geo-scientific data of geological survey of India. The geomorphology classes present in the study area are Highly Dissected Denudational Hills and Valleys, River, Highly Dissected Structural Hills and Valleys, Pediment Pediplain Complex, Active Flood Plain, Moderately Dissected Structural Hills and Valleys, Dam and Reservoir, Active Quarry, Pond, Moderately Dissected Denudational Hills and Valleys, Low Dissected Structural Hills and Valleys, Water bodies, unclassified and Abandoned Quarry

4.7. Soil: Soil map gives the soil type, which helps to understand the soil texture, permeability and cohesion, vital for determining slope stability under various loading conditions. Loose soils with poor drainage are particularly landslide-prone (Sidle & Ochiai, 2006). Soil map was prepared using soil data

from the BhuKosh. The soil map was classified based on FAO soil code as Ap21-2b (Sandy clay loam), Nd48-2/3b (Clay loam), Ah11-2c (Loam), I-Nd-c (Loam), Nd49-2bc (Loam) and Nd2-2b (Loam).

4.8. Land Use/Land Cover (LULC): LULC map depicts vegetation cover, built-up areas and bare lands, which influence runoff, erosion, and slope stability. Changes in LULC often escalate landslide susceptibility (Glade, 2003). Classified landuse map was derived from the landsat8 earthexplorer. Water, forest, flooded vegetation, crops, built area, bare ground and range land are the classes present in land use / land cover in the study area.

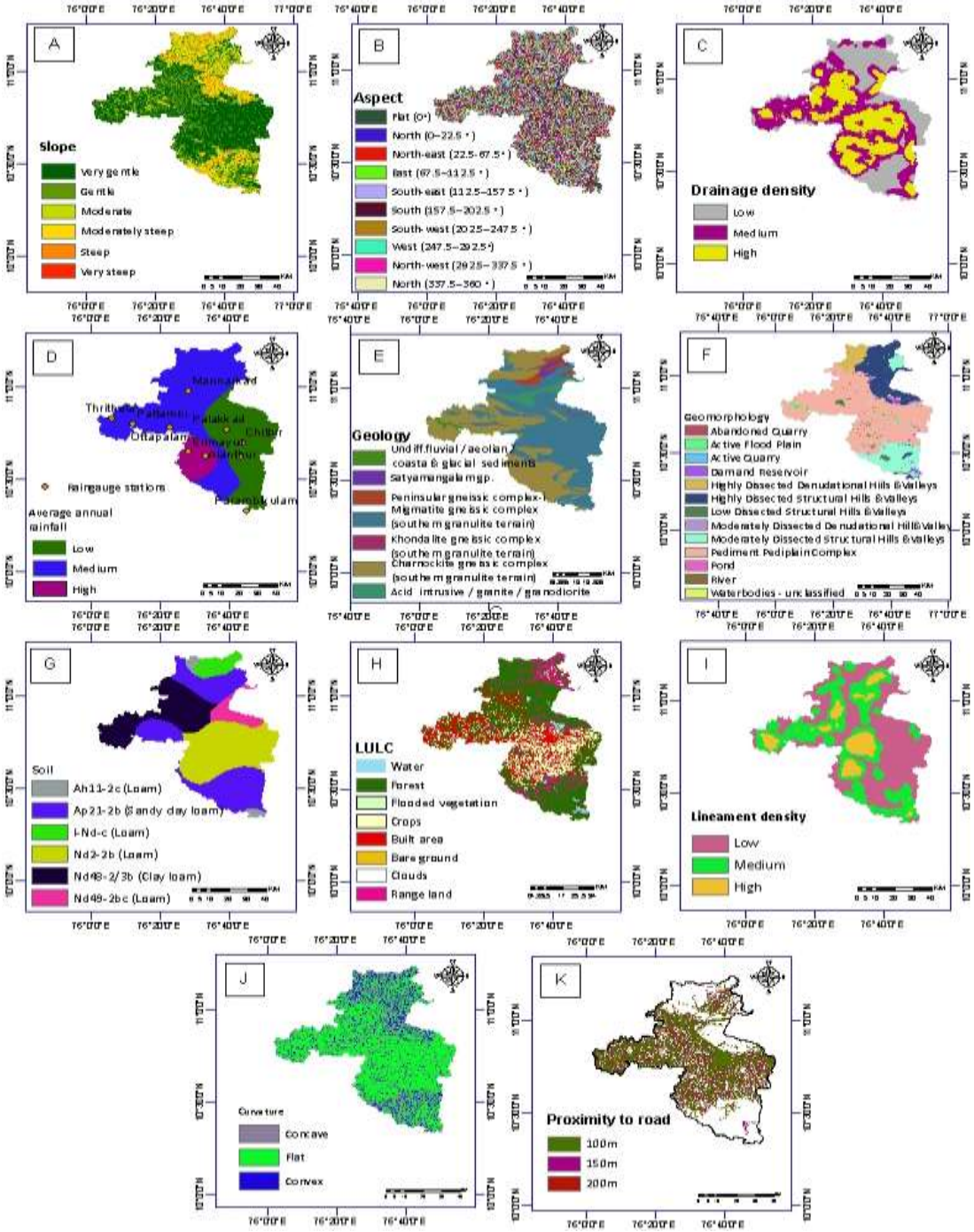

Fig.3. Landslide conditioning factors: A-slope, B-aspect, C-drainage density, D-rainfall, E-geology, F-geomorphology, G-soil, H-LULC, I-lineament density, J-curvature, K-proximity to road

4.9. Lineament density: Lineament density is the density of the linear geological structures that are expressions of underlying geological structures such as faults and fractures, present in each area. Lineament shape file was derived by interpreting the faults, fractures and the linear features across the

region. Lineament was given as input to line density tool to generate the lineament density map and classified as low, medium and high.

4.10. Curvature: Curvature map is a texture that stores the convexity/concavity of the mesh, which affecting water accumulation and soil movement. Concave slopes favor water retention, increasing saturation and instability (Meunier et al., 2008). The curvature map was generated from DEM and classified as flat, concave and convex.

4.11. Road Network: Road plays a major role in landslide susceptibility since the road alters the natural slopes, leading to destabilization (Loye et al., 2009). The construction activities carried out towards road formation like cutting and drilling weakens the bed rock and the soil above making it more susceptible to landslides. The road map obtained from the bbbike extract. It was buffered with 100, 150 and 200m interval to study the impact of roads on landslides.

5. METHODS

5.1. Frequency Ratio (FR)

The **Frequency Ratio (FR)** model is a widely used statistical technique for landslide susceptibility mapping, primarily due to its simplicity and effectiveness in assessing the relationship between landslide occurrence and various influencing factors. The method involves calculating the ratio of the frequency of landslides in specific class of a factors (e.g., slope angle, soil type, land use) to the frequency of those class in the entire area.

The Frequency Ratio for each factor class (i) is computed as:

$$FR_i = (A_i / A) \div (B_i / B) \quad \text{(1)}$$

Where:

- A_i is the number of landslides within the i-th factor class.
- A is the total number of landslides.
- B_i is the number of pixels within the i-th factor class in the entire study area.
- B is the total number of pixels in the entire study area.

The resulting frequency ratio for each class indicates the relative likelihood of landslides occurring under specific class. A higher frequency ratio signifies a higher likelihood of landslides occurring in that class, while a lower ratio indicates lower susceptibility to landslides.

5.2. Dempster-Shafer Theory of Evidence (DST)

The **Dempster-Shafer Theory of Evidence (DST)** is a mathematical framework for reasoning with uncertainty, applied in landslide susceptibility mapping to integrate multiple sources of evidence and handle incomplete or conflicting data (Dempster, A. P. 1967). DST allows the combination of information from various factors (e.g., slope, rainfall, soil type) to quantify the belief in the likelihood of landslide occurrence, considering the inherent uncertainty. Unlike traditional probability theory, DST assigns belief to evidence without requiring strict assumptions of independence, making it more flexible in modeling complex, uncertain geospatial data.In DST, evidence is represented by a basic probability assignment (BPA), which quantifies the degree of belief that a particular factor contributes to a landslide event. Each factor class (e.g., a specific slope range or land cover type) is assigned a BPA that reflects the degree of certainty in its association with landslides. The **belief** (Bel), **disbelief** (Dis), **uncertainty** (Unc) and **plausibility** (Pls) functions are central to DST and are computed as follows:

- **Belief (Bel)**: The belief function quantifies the support that the evidence provides to a specific hypothesis, calculated as the sum of BPAs over subsets of the hypothesis. The formula for belief is:

$$Bel(A) = \sum(B \subseteq A)\, m(B) \quad \text{(2)}$$

where m(B) is the basic probability assignment for subset B of hypothesis A.

- **Disbelief (Dis)**: The disbelief function quantifies the support against a hypothesis, calculated as the sum of BPAs for all subsets that do not support A. The formula for disbelief is:

$$Dis(A) = \sum(B \cap A = \emptyset)\, m(B) \quad \text{(3)}$$

- **Uncertainty (Unc)**: The uncertainty function represents the degree to which no definitive belief can be made about a hypothesis, calculated as the total BPA that is not assigned to any specific hypothesis:

Unc(A) = 1 - Bel(A) - Dis(A) ---------- (4)

- Furthermore, **Plausibility (Pls)** is a measure of the potential that a hypothesis could be true, defined as the complement of disbelief:

Pls(A) = 1 - Dis(A) ---------- (5)

DST is particularly advantageous in mapping the landslide susceptibility mapping because it can integrate different factor layers, such as slope, rainfall, soil properties, and geological factors each contributing different levels of certainty about landslide occurrence.

Table.1. Spatial association of each conditioning factor and landslide by FR and DST co-efficient.

Factors	Classes	No. of Landslide	Class pixels	FR ratio	Bel	Dis	Unc	Pls
Slope	0 - 3 % (Very gentle)	17	2156458	0.0636	0.0040	0.2266	0.7694	0.7734
	3 - 8 % (Gentle)	27	1162098	0.1875	0.0118	0.1963	0.7919	0.8037
	8 - 18 % (Moderate)	93	634660	1.1828	0.0744	0.1632	0.7624	0.8368
	18 - 30% (Moderately steep)	194	517632	3.0251	0.1905	0.1285	0.6810	0.8715
	30 - 50% (Steep)	241	277052	7.0212	0.4423	0.1105	0.4473	0.8895
	> 50 % (Very steep)	21	38528	4.3995	0.2770	0.1750	0.5480	0.8250
Aspect	Flat (0°)	62	529565	0.9450	0.0959	0.1001	0.8040	0.8999
	North (0–22.5 °)	46	396384	0.9367	0.0951	0.1016	0.8034	0.8984
	North-east (22.5-67.5 °)	39	397708	0.7915	0.0803	0.1029	0.8168	0.8971
	East (67.5–112.5 °)	47	466126	0.8139	0.0826	0.1022	0.8152	0.8978
	South-east (112.5–157.5 °)	92	537068	1.3827	0.1403	0.0945	0.7652	0.9055
	South (157.5–202.5 °)	89	591165	1.2152	0.1233	0.0956	0.7810	0.9044
	South-west (202.5–247.5 °)	46	499983	0.7426	0.0754	0.1027	0.8219	0.8973
	West (247.5–292.5°)	45	420938	0.8629	0.0876	0.1020	0.8104	0.8980
	North-west (292.5–337.5 °)	61	465984	1.0566	0.1072	0.0996	0.7932	0.9004
	North (337.5–360 °)	66	481507	1.1064	0.1123	0.0988	0.7889	0.9012
Drainage density	Low	297	8970	1.5928	0.5411	0.2465	0.2124	0.7535

	Medium	245	10818	1.0894	0.3661	0.3020	0.3319	0.6980
	High	51	8738	0.2808	0.0928	0.4515	0.4557	0.5485
Rainfall	Low	201	10094	1.0116	0.4114	0.3410	0.2476	0.6590
	Medium	373	17322	1.0939	0.4456	0.2234	0.3310	0.7766
	High	19	2709	0.3563	0.1430	0.4355	0.4214	0.5645
Geology	Satyamangalam gp.	4	341	0.5984	0.0514	0.1571	0.7916	0.8429
	Peninsular gneissic complex-i	5	1021	0.2498	0.0213	0.1587	0.8201	0.8413
	Migmatite gneissic complex (southern granulite terrain)	247	15388	0.8189	0.0706	0.1232	0.8062	0.8768
	Charnockite gneissic complex (southern granulite terrain)	325	12029	1.3783	0.1201	0.0885	0.7913	0.9115
	Khondalite gneissic complex (southern granulite terrain)	8	56	7.2879	0.7211	0.1553	0.1236	0.8447
	Acid intrusive / granite / granodiorite	4	1122	0.1819	0.0155	0.1592	0.8253	0.8408
	Undiff.fluvial / aeolian / coasta & glacial sediments	0	295	0.0000	0.0000	0.1580	0.8420	0.8420
Geomorphology	Highly Dissected Denudational Hiils and Valleys	158	1598	5.0441	0.3844	0.0599	0.5557	0.9401
	River	1	256	0.1993	0.0137	0.0799	0.9064	0.9201
	Highly Dissected Structural Hills and Valleys	112	5491	1.0406	0.0729	0.0711	0.8560	0.9289
	Pediment Pediplain Complex	35	17150	0.1041	0.0072	0.1054	0.8874	0.8946
	Active Flood Plain	0	426	0.0000	0.0000	0.0803	0.9197	0.9197
	Moderately Dissected Structural Hills and Valleys	268	4401	3.1066	0.2271	0.0469	0.7259	0.9531

	Dam and Reservoir	1	391	0.1305	0.0090	0.0801	0.9109	0.9199
	Active Quarry	0	21	0.0000	0.0000	0.0797	0.9203	0.9203
	Pond	0	6	0.0000	0.0000	0.0797	0.9203	0.9203
	Moderately Dissected Denudational Hills and Valleys	3	72	2.1256	0.1523	0.0794	0.7683	0.9206
	Low Dissected Structural Hills and Valleys	15	409	1.8710	0.1334	0.0782	0.7884	0.9218
	Waterbodies – unclassified	0	26	0.0000	0.0000	0.0797	0.9203	0.9203
	Abandoned Quarry	0	5	0.0000	0.0000	0.0797	0.9203	0.9203
Soil	Ap21-2b (Sandy clay loam)	425	10008	2.1099	0.3314	0.0627	0.6059	0.9373
	Nd48-2/3b (Clay loam)	41	6757	0.3015	0.0456	0.1945	0.7599	0.8055
	Ah11-2c (Loam)	11	617	0.8858	0.1356	0.1832	0.6812	0.8168
	I-Nd-c (Loam)	4	1579	0.1259	0.0190	0.1886	0.7925	0.8114
	Nd49-2bc (Loam)	90	1585	2.8212	0.4499	0.1608	0.3893	0.8392
	Nd2-2b (Loam)	22	8917	0.1226	0.0185	0.2102	0.7713	0.7898
Landuse/ Landcover	Water	0	744278	0.0000	0.0000	0.1374	0.8626	0.8626
	Trees	433	23824109	1.3738	0.3311	0.0501	0.6189	0.9499
	Flooded vegetation	0	3822	0.0000	0.0000	0.1363	0.8637	0.8637
	Crops	2	7531494	0.0201	0.0048	0.1483	0.8469	0.8517
	Built area	16	8598567	0.1407	0.0339	0.1467	0.8194	0.8533
	Bare ground	0	17356	0.0000	0.0000	0.1363	0.8637	0.8637
	Clouds	0	205	0.0000	0.0000	0.1363	0.8637	0.8637
	Range land	142	4104408	2.6151	0.6302	0.1086	0.2612	0.8914
Lineament density	Low	358	14550	1.1830	0.5008	0.2271	0.2721	0.7729
	Medium	222	10764	0.9916	0.4181	0.3296	0.2523	0.6704

	High	13	3197	0.1955	0.0811	0.4433	0.4756	0.5567
Curvature	Concave	185	984054	1.5226	0.3571	0.2502	0.3927	0.7498
	Flat	210	3086249	0.5511	0.1292	0.5226	0.3482	0.4774
	Convex	198	732293	2.1898	0.5137	0.2272	0.2591	0.7728
Road	100m	61	12389	2.4482	0.7168	0.1667	0.1165	0.8333
	150m	19	15933	0.5929	0.1730	0.3964	0.4306	0.6036
	200m	14	18417	0.3780	0.1102	0.4369	0.4529	0.5631

6.3. AUC-ROC Validation

The Area under the Receiver Operating Characteristic Curve (AUC-ROC) is a widely used method for validating landslide susceptibility models. In ArcGIS, the AUC-ROC is applied to evaluate the predictive accuracy of susceptibility maps by comparing predicted landslide probabilities to actual landslide occurrences. The ROC curve plots true positive rate (sensitivity) against the false positive rate (1-specificity) at various threshold settings. The AUC value quantifies the overall performance of the model, with a higher value (close to 1) indicating better predictive capability, while a value close to 0.5 suggests a model with no discriminatory power. The AUC-ROC approach is particularly useful for assessing the effectiveness of landslide susceptibility models, as it provides an objective measure of model performance, independent of specific classification thresholds.

7. RESULTS AND DISCUSSION

7.1. Landslide susceptibility model analysis for FR and DST

The FR model establishes a relationship between landslide occurrences and associated causative factors. Each factor is categorized into distinct classes and for each classes, the number of landslide pixels, total class pixels and the resulting frequency ratio (FR) are calculated. The FR value quantifies the likelihood of landslide occurrence relative to the spatial distribution of those specific factor classes, where values greater than 1 indicate a higher susceptibility. Figure 5 shows the landslide susceptibility map using FR model. The integration of the Dempster-Shafer Theory of Evidence (DST) with the Frequency Ratio (FR) model provides a probabilistic framework to evaluate landslide susceptibility by incorporating uncertainty and evidence-based reasoning.

DST allows mapping the degree of belief, disbelief, plausibility, and uncertainty for each factor class, complementing the deterministic nature of the FR model. Belief represents the minimum degree of support or confidence for a specific factor class contributing to landslide susceptibility. Disbelief quantifies the degree to which evidence contradicts a class's contribution to landslide susceptibility. Plausibility represents the upper limit of belief, accounting for uncertainty. It combines the degree of belief and uncommitted evidence, providing a broader range for decision-making. Uncertainty captures the lack of conclusive evidence, balancing belief and disbelief. This hybrid method enables a more robust and comprehensive evaluation of landslide susceptibility. Figure 6 shows the landslide susceptibility maps using DST model. This detailed assessment of spatial relationships between landslides and causative factors provides a robust foundation for landslide susceptibility mapping, enabling researchers and policymakers to prioritize high-risk areas for preventive measures and sustainable land-use planning.

7.1.1. Slope: Steep slopes (30–50%) show the highest landslide frequency, with 241 landslide pixels and an FR of 7.0212, followed by moderately steep slopes (18–30%) with 194 landslide pixels (FR 3.0251). Very gentle slopes (0–3%) have the lowest landslide occurrences (17 pixels, FR 0.0636), making them the most stable. DST confirms this trend, with steep slopes showing high belief (0.4423) and plausibility (0.8895), while gentle slopes have negligible belief (0.0040). FR assigns higher weights to slope classes

with more observed landslides where DST considers that steep slopes may not always trigger landslides if vegetation or rock type resists failure. It assigns partial belief to multiple slope classes and integrates other evidence like geology and land use.

7.1.2. Aspect: The southeast-facing slopes (112.5–157.5°) have the highest landslide occurrence, with 92 out of 593 landslides and FR of 1.3827, highlighting their susceptibility to landslide. The south-facing slopes (157.5–202.5°) follow closely with 89 landslides (FR 1.2152). Conversely, flat terrain exhibits the lowest susceptibility, with only 62 landslides (FR 0.79). DST analysis confirms that southeast-facing slopes have the highest plausibility (0.9055), while flat areas exhibit significant uncertainty (0.8040). FR only considers the direction that historically had more landslides but DST accounts for uncertainty due to variable sun exposure, wind and moisture on different slopes, especially when orientation effects vary seasonally or topographically.

7.1.3. Drainage Density: In contrast, to the other works in the literature low drainage density areas dominates landslide occurrences with 297 landslides and an FR of 1.5928, indicating that the drainage density does not contribute to landslides in this study area. Medium-density areas have 245 landslides (FR 1.0894). High-density regions contribute only 51 landslides (FR 0.2808). DST analysis also presents the similar results, with low-density regions showing the highest belief (0.5411), while high-density areas have a high disbelief (0.4515) and uncertainty (0.4557). DST recognizes that drainage effects are nonlinear and location dependent. i.e., high drainage density in rocky terrain might be less dangerous than weathered soil.

7.1.4. Rainfall: Medium rainfall zones (2031 -2300 mm) account for the most landslide pixels (373) with an FR of 1.0939, followed by low rainfall areas (201 landslide pixels, FR 1.0116). Even though it is categorized as Low rainfall class it receives an average annual rainfall between 1600 – 2300 mm. surprisingly, high rainfall areas show only 19 landslide pixels (FR 0.3563), indicating other stabilizing factors like vegetation or drainage. DST analysis aligns with this, showing medium rainfall zones with the highest plausibility (0.7766) and high rainfall areas with high uncertainty (0.4214). DST handles missing or inconsistent rainfall values and still contributes plausible risk to certain areas without over committing to unreliable data.

7.1.5. Geology: The Khondalite Gneissic Complex is the most susceptible, with 325 landslide pixels and an FR of 7.2879. The Migmatite and Charnockite Gneissic Complexes have moderate FR values (0.8189 and 1.3783 respectively), while the Satyamangalam Group and Peninsular Gneissic Complex-I exhibit low susceptibility with FR 0.5984 and 0.2498, respectively. DST results indicate Khondalite Gneissic Complex has the highest belief (0.7211), while acid intrusive formations have low belief (0.0155) and high disbelief (0.1592).

7.1.6. Geomorphology: Highly dissected denudational hills and valleys show the highest landslide occurrences (158 landslides and FR 5.0441), while moderately dissected structural hills and valleys have 268 landslides (FR 3.1066). Lowland flood plains and river corridors exhibit minimal susceptibility, with very low or zero FR values. DST analysis shows high belief for dissected hills and valleys, reinforcing their landslide vulnerability. FR uses categorical class frequency but DST assigns partial belief to units where terrain transitions occur and integrate with other evidence for refined susceptibility.

7.1.7. Soil: The sandy clay loam class of soil has the highest landslide occurrence (425 pixels, FR 2.1099), followed by loam with 2.8212 FR. Sandy clay loam is more susceptible to landslide because the sand content makes it is less cohesive and the clay content tends to hold more water and increase the weight of the soil. Other soil types such as Nd48-2/3b (clay loam) and Ah11-2c (loam) have lower FR values, making them relatively more stable. DST analysis confirms that sandy clay loam has a high belief value, suggesting its susceptibility to failure under adverse conditions.

7.1.8. Land Use/ Land cover: Forest areas have the highest landslide occurrence (433 landslides, FR 1.3738). The forest area is usually less prone to landslides due to their strong root network system but in this study area majority of the landslides are present in the forest region mainly due to the reason that the entire forest region falls under the moderately steep and steep region. Next to forest range land has the highest landslides (142 landslides). The built-up areas contribute minimal landslides (FR 0.1407). In DST model the range land has the highest belief value of 0.6302 followed by forest areas. The range lands

are mainly covered by grass which has a weaker root system and make the soil more susceptible to erosion and thereby susceptible to landslides.

7.1.9. Lineament Density: Low lineament density regions have the highest landslide occurrences (358 landslide pixels, FR 1.1830), while medium density follows with 222 landslide pixels (FR 0.9916). High-density areas have the least landslides (FR 0.1955), implying that high structural discontinuity may not necessarily correlate with instability. DST results align with this, showing low-density regions with higher belief values. DST captures the indirect role of fractures and fault systems more realistically by combining lineament data with slope, geology, and drainage information using belief modeling.

7.1.10. Curvature: Convex regions exhibit the highest landslide susceptibility (198 landslides, FR 2.1898), while concave regions have a moderate landslide frequency (185 landslides, FR 1.5226). Flat areas dominate in terms of spatial coverage but have a lower landslide frequency (210 pixels, FR 0.5511). DST analysis reinforces this, with convex surfaces showing higher belief values. Surface curvature often has context-dependent effects i.e., concave in clay-rich soils is more dangerous than in rocky slopes. DST accounts for such interaction effects by integrating multiple evidence sources.

7.1.11. Proximity to Roads: Areas within 100m of roads have the highest landslide occurrences (94 landslides, FR 2.4482), while susceptibility decreases with distance 150m (FR 0.5929) and 200m (FR 0.3780). This suggests human-induced disturbances play a significant role in slope destabilization. DST confirms this trend, showing higher belief values near roads and reduced influence further away. It models the indirect effects of roads (e.g., water seepage, vibration, slope cutting) by combining with slope, drainage, and soil data offering a more realistic susceptibility assessment.

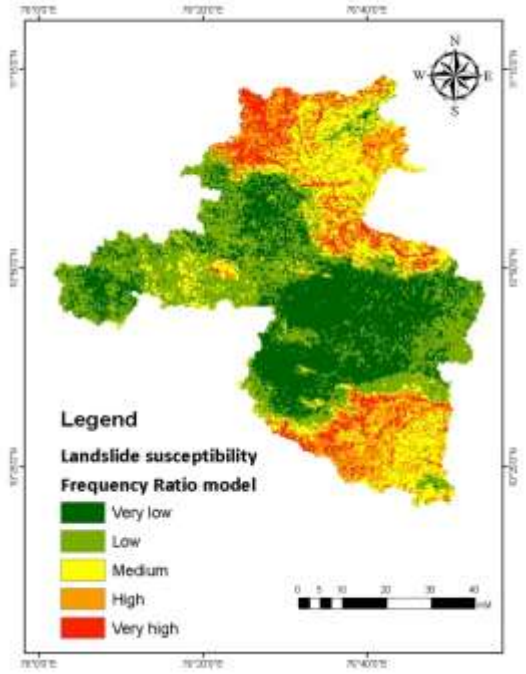

Fig.5. Landslide susceptibility map using FR model

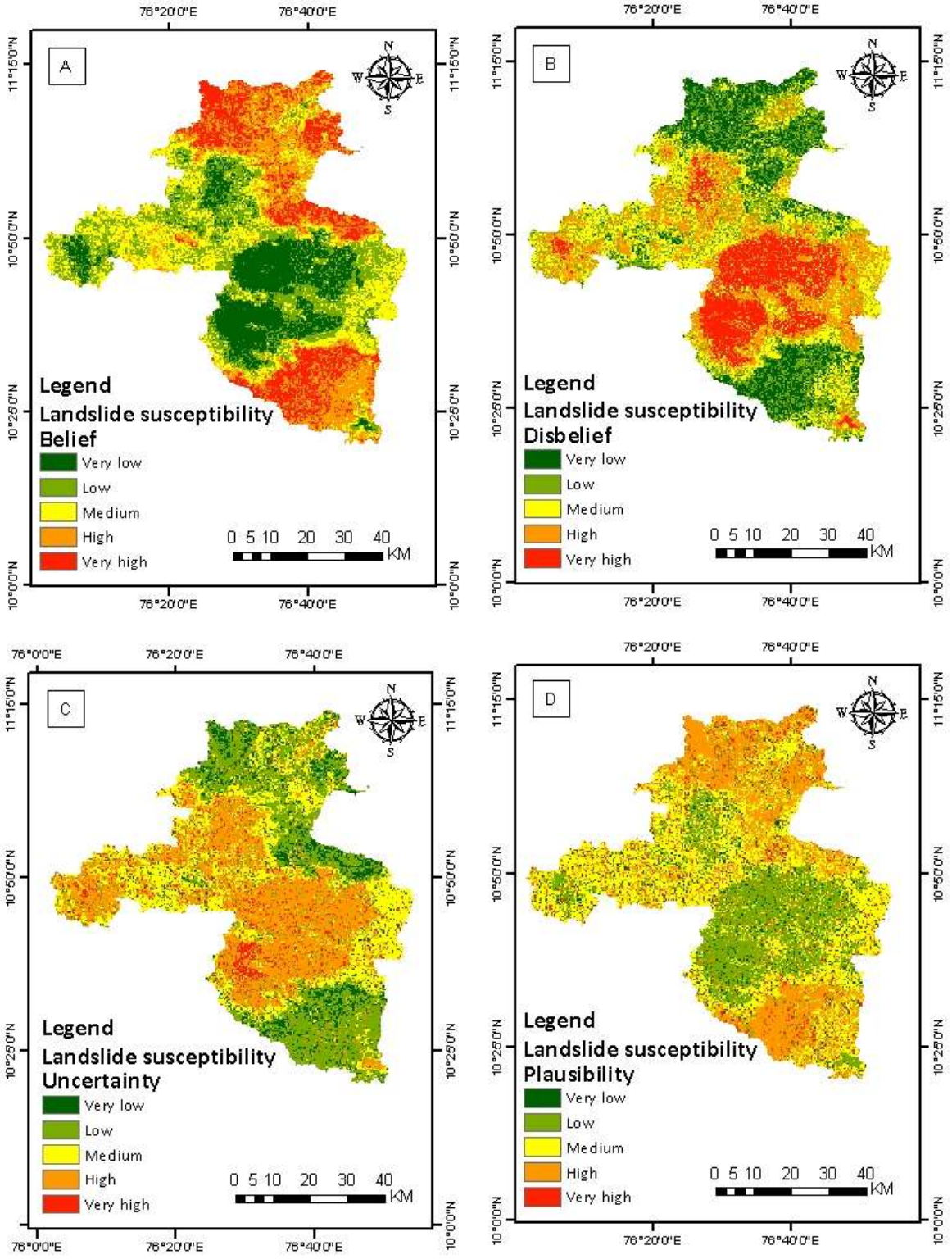

Fig.6. Landslide Susceptibility maps using DST model: A-belief, B-disbelief, C-uncertainty, and D-plausibility

The landslide susceptibility in Palakkad District is categorized into five levels: Very Low, Low, Moderate, High, and Very High, using both Frequency Ratio and Dempster-Shafer Theory of Evidence. The Frequency Ratio indicates the total area (in km²) under each susceptibility level, with the largest areas

classified as Low (1357 km²) and Very Low (1338 km²), while the Very High susceptibility zone covers only 315 km². 732 numbers of settlements were mapped in the base map. In landslide susceptibility map from frequency ratio method out of 732 settlements 14 settlements fall under moderate susceptibility class and 3 settlements fall under high susceptibility class. No settlement was found in very high susceptibility class.

Belief values represent areas with strong evidence supporting the classification, showing that Moderate (1020 km²) and High (961 km²) susceptibility zones have higher certainty compared to Very High (681 km²). Conversely, Disbelief values highlight areas where classification is uncertain or contradictory, with High (1400 km²) and Moderate (1170 km²) zones having significant disagreement. The Uncertainty metric shows the extent of ambiguity in classification, with Moderate (1599 km²) and High (1305 km²) areas having the highest uncertainty, indicating the need for further validation. Lastly, Plausibility reflects the possible extent of each susceptibility level, with the Moderate category having the highest plausible extent (1599 km²), whereas the Very High category remains the lowest at 249 km². These variations suggest that while certain areas have strong classification confidence, others require further investigation for precise risk assessment. In this model, out of 732 settlements 186 settlements fall under moderate susceptibility class, 16 settlements fall under high susceptibility class and 2 settlements (Nelliyampathy and Nooradipalam) fall under very high susceptibility class.

7.2. Validation of Landslide Susceptibility Mapping

The accuracy assessment of landslide susceptibility mapping was conducted using the Area Under the Curve (AUC) method. Figure 7 represents the landslide susceptibility map using Frequency Ratio (FR) model, which achieved an AUC value of 85%, indicating a relatively high predictive capability for landslide-prone areas. This suggests that the FR model effectively captures the relationship between conditioning factors and landslide occurrences, making it a reliable approach for susceptibility mapping. The Dempster-Shafer (DS) model provided a more comprehensive probabilistic assessment of landslide susceptibility (Figure 8). The landslide susceptibility map using belief value showed an accuracy of 95%, reflecting strong confidence in the model's ability to predict landslide-prone areas. The disbelief map showed an accuracy of 37%, indicating some level of uncertainty and potential misclassification in specific regions. The uncertainty and plausibility values both stood at 70%, suggesting a significant degree of variability in the model's assessment. The high uncertainty indicates that additional data or refinement in factor weightings might be required to further improve the model's reliability.

7.3. Comparative Analysis of Models

The comparison between the FR and DS models highlights the strengths and limitations of each approach. The FR model, with its 85% AUC accuracy, provides a relatively straightforward and effective method for landslide susceptibility mapping. However, it lacks the ability to incorporate uncertainty explicitly. On the other hand, the DS model, with its 95% accuracy for belief value, offers a more detailed probabilistic interpretation, which can be useful in decision-making scenarios where uncertainty needs to be accounted for. The relatively high disbelief (37%) and uncertainty (70%) in the DS model suggest that while it provides a robust assessment, further refinement in input parameters or additional validation may be necessary to enhance its predictive accuracy.

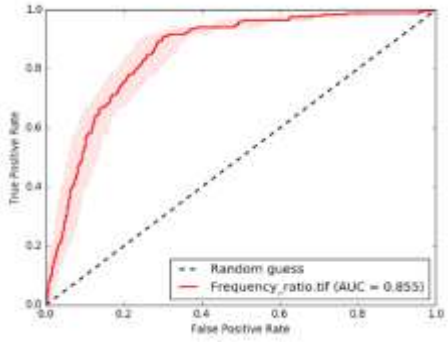

Fig.7. Receiver operating characteristics ROC curve for FR model

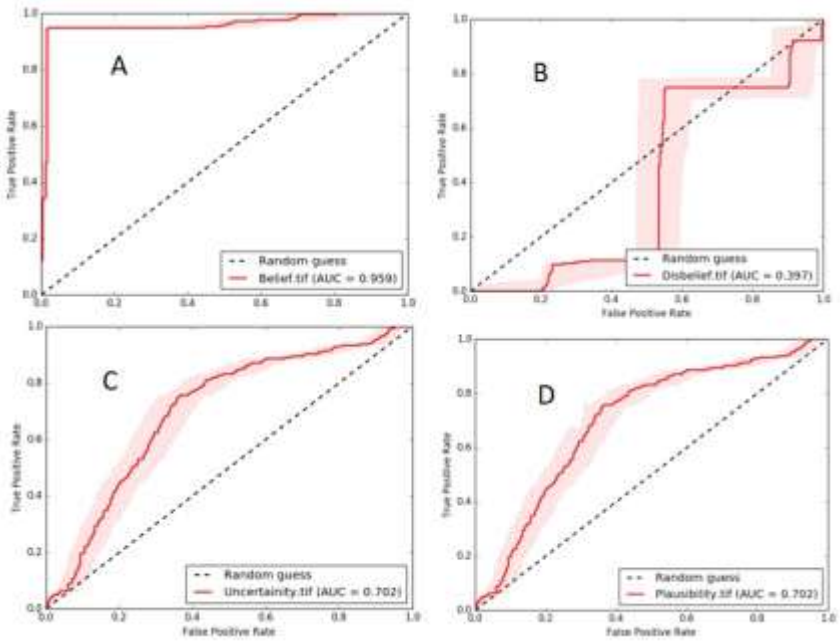

Fig.8. Receiver operating characteristics ROC curve for DST model: A-belief, B-disbelief, C-uncertainty, D-plausibility

8. CONCLUSION

The study on Landslide Susceptibility Mapping in Palakkad District demonstrates the effectiveness of both the Frequency Ratio (FR) and Dempster-Shafer (DS) models in predicting landslide-prone areas. The FR model, with an AUC accuracy of 85%, serves as a simple and reliable tool for susceptibility assessment; the Dempster-Shafer Theory of Evidence model proves to be more effective due to its probabilistic approach, achieving an accuracy of 95%. The DS model's ability to quantify uncertainty makes it particularly advantageous in handling complex terrain conditions and incomplete data, a crucial aspect in landslide prediction. Unlike the FR model, which relies purely on statistical correlations, the DS model incorporates uncertainty measures, making it more robust in decision-making scenarios where data inconsistencies exist. This probabilistic advantage allows for a more refined classification of susceptibility zones, reducing false positives and enhancing predictive accuracy. Overall, the results underscore the importance of integrating multiple models for a comprehensive landslide susceptibility assessment. However, given its superior ability to manage uncertainty and provide a more detailed probabilistic interpretation, the DS model emerges as a more effective tool for landslide prediction. These findings can aid policymakers and local authorities in implementing targeted and data-driven disaster management strategies to mitigate landslide risks in Palakkad District.

REFERENCES

[1] Guzzetti, F., Reichenbach, P., Cardinali, M., Galli, M., and Ardizzone, F., 2005, "Landslide Hazard Assessment in Areas of Low Information Availability," *Earth-Sci. Rev.*, 79(3–4), pp. 271–303. https://doi.org/10.1016/j.earscirev.2006.04.002

[2] Dai, F. C., Lee, C. F., and Ngai, Y. Y., 2002, "Landslide Risk Assessment and Management: An Overview," *Geomorphology*, 66(1–4), pp. 31–54. https://doi.org/10.1016/S0169-555X(02)00060-X

[3] Aleotti, P., and Chowdhury, R., 1999, "Landslide Hazard Assessment: Summary Review and New Perspectives," *Eng. Geol.*, 55(3), pp. 227–249. https://doi.org/10.1016/S0013-7952(99)00078-1

[4] Sarkar, S., Kanungo, D. P., Patra, A. K., and Kumar, P., 2012, "GIS-Based Landslide Susceptibility Assessment Using Analytical Hierarchy Process (AHP): A Study on the National Highway-58, India," *Nat. Hazards*, 59(3), pp. 1255–1275. https://doi.org/10.1007/s11069-011-9831-z

[5] Chen, W., Li, Y., Chai, H., and Hou, E., 2017, "GIS-Based Landslide Susceptibility Modeling: A Comparative Assessment of Frequency Ratio, Statistical Index, and Weights of Evidence Models," *Nat. Hazards*, 89(2), pp. 641–662. https://doi.org/10.1007/s11069-017-2989-y

[6] Pradhan, B., 2010, "Landslide Susceptibility Mapping of a Catchment Area Using Frequency Ratio, Fuzzy Logic, and Multivariate Logistic Regression Approaches," *J. Indian Soc. Remote Sens.*, 38(2), pp. 301–320. https://doi.org/10.1007/s12524-010-0020-z

[7] Pourghasemi, H. R., Pradhan, B., and Gokceoglu, C., 2012, "Application of Weights-of-Evidence and Certainty Factor Models and Their Comparison in Landslide Susceptibility Mapping at Haraz Watershed, Iran," *Geomatics, Nat. Hazards Risk*, 3(2), pp. 149–163. https://doi.org/10.1080/19475705.2011.560789
[8] Lee, S., and Talib, J. A., 2005, "Probabilistic Landslide Susceptibility and Factor Effect Analysis," *Environ. Geol.*, 47(7), pp. 982–990. https://doi.org/10.1007/s00254-005-1228-z
[9] Shibu, T. M., and Nair, P., 2016, "Landslide Susceptibility Analysis of Western Ghats, Kerala, India," *Int. J. Environ. Res. Dev.*, 6(4), pp. 289–299.
[10] Sreekumar, M., Muraleedharan, P., and George, T., 2017, "Geology and Landslide Susceptibility Mapping of Palakkad District, Kerala," *J. Geosci. Environ. Prot.*, 5(5), pp. 173–182. https://doi.org/10.4236/gep.2017.55012
[11] Nair, R. K., and Srinivasan, K., 2020, "Hydro-Meteorological Factors Influencing Landslides in the Western Ghats," *Hydrol. Res.*, 51(3), pp. 520–533. https://doi.org/10.2166/nh.2020.023
[12] Menon, M., Krishnan, S., and Kumar, A., 2018, "Rainfall-Induced Landslides in the Western Ghats, India: A Geomorphological Perspective," *Nat. Hazards*, 93(3), pp. 1167–1182. https://doi.org/10.1007/s11069-018-3314-2
[13] Thomas, J., Joseph, S., and George, S., 2015, "Deforestation and Its Role in Landslide Occurrences in Kerala," *J. Earth Sci.*, 67(2), pp. 34–41.
[14] Paul, R., and Mathew, T., 2019, "Landslide Hazards in the Nelliampathy Hills: A Case Study," *Nat. Hazards Rev.*, 20(4), 04019006. https://doi.org/10.1061/(ASCE)NH.1527-6996.0000338
[15] Vinod, K. S., and Shetty, N., 2021, "Anthropogenic Impact on Landslide Susceptibility in Palakkad, Kerala," *Environ. Earth Sci .*, 80(5), 245. https://doi.org/10.1007/s12665-021-09576-y
[16] Gupta, S., and Rajagopal, R., 2019, "Urbanization and Landslide Risk in the Indian Context," *Landslide Risk Assess.*, 12(1), pp. 45–60.
[17] Ayalew, L., Yamagishi, H., and Ugawa, N., 2004, "Landslide Susceptibility Mapping Using GIS-Based Weighted Linear Combination, the Case in Tsugawa Area of Agano River, Niigata Prefecture, Japan," *Geomorphology*, 65(1–2), pp. 15–31. https://doi.org/10.1016/j.geomorph.2003.10.013
[18] Regmi, N. R., Giardino, J. R., and Vitek, J. D., 2014, "Assessing Susceptibility to Landslides: Using Models to Understand Observed Landslide Processes for Future Land-Use Planning," *Geomorphology*, 226, pp. 103–120. https://doi.org/10.1016/j.geomorph.2013.12.004
[19] Gokceoglu, C., and Aksoy, H., 1996, "Landslide Susceptibility Mapping of the Slopes in the Residual Soils of the Mengen Region (Turkey) by Deterministic Stability Analyses and Image Processing Techniques," *Geomorphology*, 20(4), pp. 317–328. https://doi.org/10.1016/0169-555X(96)00023-9
[20] Crozier, M. J., 2010, "Deciphering the Effect of Climate Change on Landslide Activity: A Review," *Geomorphology*, 124(3–4), pp. 260–267. https://doi.org/10.1016/j.geomorph.2009.01.003
[21] Soeters, R., and van Westen, C. J., 1996, "Slope Instability Recognition, Analysis, and Zonation," in Turner, A. K., and Schuster, R. L., Eds., *Landslides: Investigation and Mitigation*, National Academy Press, Washington, DC, pp. 129–177. https://doi.org/10.1016/0169-555X(95)00069-0
[22] Sidle, R. C., and Ochiai, H., 2006, *Landslides: Processes, Prediction, and Land Use*, Cambridge University Press. https://doi.org/10.1017/CBO9780511735482
[23] Glade, T., 2003, "Landslide Occurrence as a Response to Land Use Change: A Review of Evidence from New Zealand," *Caterbury Res. J.*, 32(4), pp. 205–219. https://doi.org/10.1016/S0264-8172(03)00038-2
[24] Meunier, P., Hovius, N., and Haines, J. A., 2008, "Topographic Site Effects and the Location of Earthquake-Induced Landslides," *Earth Planet. Sci. Lett.*, 275(3–4), pp. 221–232. https://doi.org/10.1016/j.geomorph.2008.03.011
[25] Loye, A., Jaboyedoff, M., and Pedrazzini, A., 2009, "Identification of Potential Rockfall Source Areas at a Regional Scale Using a DEM-Based Geomorphometric Analysis," *Geomorphology*, 110(3–4), pp. 98–112. https://doi.org/10.1016/j.geomorph.2008.08.001
[26] Dempster, A. P., 1967, "Upper and Lower Probabilities Induced by a Multivalued Mapping," *Ann. Math. Stat.*, 38(2), pp. 325–339. https://doi.org/10.1214/aoms/1177698950